International Journal of Research in Science and Technology

Volume 12, Issue 04: October-December 2025

ISSN 2394 - 9554

A Simple Oil-Water Experiment to Verify Oil Quality

Kalimuthu Swaminathan,*
Department of Automobile Engineering, PSG College of Technology, Coimbatore, India

*E-mail: swamiooty@yahoo.com

Abstract

Natural oil films and their dynamics on water are interesting to many applications like oil spills on sea and in coating stability. The dynamics of such natural oil films on water is the subject of this experimental study. In this paper a simple oil-water dynamics experiment is proposed to identify oil type and quality, by characterizing the spreading and dewetting process of an oil film on water. Experiments have been performed with gingelly oil, olive oil, castor oil and coconut oil. In each experiment a drop of test fluid (one of the natural oils) is placed gently on the surface of water. The spreading patterns of the oil film was recorded was recorded and analyzed. In all cases, it was observed that the natural oil drop spreads spontaneously on the free surface of water. Subsequently, number of holes are observed to form on the spreading front of oil film. When the hole count reaches the particular limit called random packing limit, holes start to merge with the adjacent holes, and this process continues and results to a coarser structure of the oil films. This process is quantified initially using spreading rate. The general path traced by the centroid were also shows a radially outward. Therefore, the spreading and hole formation process is modelled using potential flow theory. Pseudo color images of the all the modelled holes predicting the movement of the spreading front meniscus to some extent. Furthermore, It was also found that the all the measure of holes displacement shows an increase in randomness as the holes count reaches towards random packing limit.

Keywords: *Spreading, Hole nucleation, Hole Growth, Hole Coalescence, film coarsening, Oil quality, miscible constituents.*

1. INTRODUCTION

Natural oils are important to nutrition, Biodiesel and several other industrial applications. The presence of unsaturated compounds in the natural oils are well correlated with the cholesterol level. The quality of natural oil quantity depends on the amount of unsaturated compounds in the oil[2]. If the unsaturated compounds percentage is more, then oil ages in accelerated manner. Several applications rely on high and reproducible quality of these natural oils. An industry standard quality control tool is Gas Chromatography and Mass Spectrometry (GCMS). GCMS yields the chemical composition of a material. In the context of oils, GCMS can only be used after esterification, where the fatty acid triglycerides are first converted to their esters. In many instances, this may not be possible. In addition, it may be useful to develop a quick tool which will allow for identification of an oil and verify adulteration as shown by Babu et al[3], rather than the detailed composition. Oxidation of natural oil also occurs due to the presence more unsaturated compounds, i.e. Number of double bond and the position of the double bond in the fatty acid chain. Because of this oxidation problem, most of the natural oil cannot be stored for more than 1 year. Furthermore natural oil quality is also important in the food industry. For

https://doi.org/10.64151/PSGCARE-13

ISSN 2394 - 9554

example, a method that could identify whether two oil samples are from the same source is certainly useful. This is a key motivation of the current work. During this work, in this paper it is shown that the certain features of the natural oil film dynamics on water can be used as markers to both identify oil as well as characterize a deviation of given oil from a standard. The dynamics of partially miscible liquids will be discussed briefly before outlining the proposed method.

Harkins et al[4] showed that the spreading process is governed by spreading coefficient (S), which is derived from the surface tensions of the spreading liquid and the substrate liquid and interfacial tension between these liquids. Let $\gamma_s$be the substrate fluid surface tension, γ_d be the surface tension of the drop liquid and γ_{ds} is the interfacial tension between drop liquid and substrate liquid. Then,$S = \gamma_s - (\gamma_{ds} + \gamma_d)$. If $S < 0$ ($S > 0$), the drop will not spread on the substrate. In the case of natural oil-water systems, the spreading coefficient S is always greater than zero. Generally, there is also loss of interfacial energy as an immiscible liquid drop spreads on another immiscible liquid substrate. Due to spreading, the energy associated with the air-water interface (or surface tension) is decreased whereas an equal amount of energy associated with the air / oil and oil / water interfaces is increased. Oil spreading on water results in the net loss of surface energy leading the drop towards a global minimum in interfacial free energy. Gravitational forces initially govern the dynamics of drop spreading until the drop becomes so thin that capillary forces dominate. The total energy during a spreading process has to be conserved i.e., the net loss of gravitational energy and surface energy has to be balanced by the net increase in other forms of energy. There is a net increase in the kinetic energy of the spreading oil drop on water substrate as well as an increase in thermal energy created by viscous forces in both the oil and water phases. Balancing these forces gives rise to the spreading laws governing system dynamics.

Harkins et al[4] have also shown that an oil drop could spread whereas the thin film remains as an intact film until it forms a monomolecular layer. However, in this case the spreading coefficient of the liquid/liquid system has to be positive and high. In addition, the spreading liquid should contain polar group molecules. Liquids like decane have low but positive spreading coefficient. These kinds of liquids spread over water surface for some time and form a thick stable film. The thickness of the film in this case, is much greater than that of a monomolecular layer. In the context of the present study, natural oil-water systems have a high positive spreading coefficient, but show both spreading and dewetting leading to hole nucleation. hole nucleation dynamics is chosen as a marker to differentiate various oils and detect adulteration.

Natural oil drops spreading on aqueous solutions is an example of a liquid/liquid system that could exhibit both wetting and dewetting processes spontaneously (without inducement) and simultaneously. These processes happening at room temperature have not been explored in the literature. The oil film evolves through following three processes: (i) spreading (where the oil film increases in diameter), (ii) hole inception and its growth (where holes are formed on the film), (iii) hole coalescence (where the oil film coarsens). Swaminathan and Panchagnula[5] have experimentally investigated the oil film dynamics on water. They showed that natural oil drop spreads on water and when the spreading oil film attains a critical film thickness, holes are formed at various places of the spreading front. They also observed that the spreading process is affected by the presence of a contaminant (Octanoic acid in this case) in the substrate. This manuscript, compares the spreading patterns of different oils. Spreading experiments has been performed with gingelly oil, olive oil, castor oil and coconut oil. It is found that each oil has a unique spreading pattern. Further coconut oil from different sources has different spreading patterns. The patterns formed by each oil will be characterized using three distinct parameters to differentiate each oil and its source.

https://doi.org/10.64151/PSGCARE-13

ISSN 2394 - 9554

EXPERIMENTAL APPARATUS AND PROCEDURE

A cylindrical container of around 20 cm inner diameter (which was coated with Teflon®)was filled with water. Water is the substrate liquid. A natural oil drop of volume, 16μl was metered using a micropipette in all experiments. Figure 1(a) shows the representation diagram of the current experimental set up. Figure 1(b) shows a raw image obtained from one of the experiments.

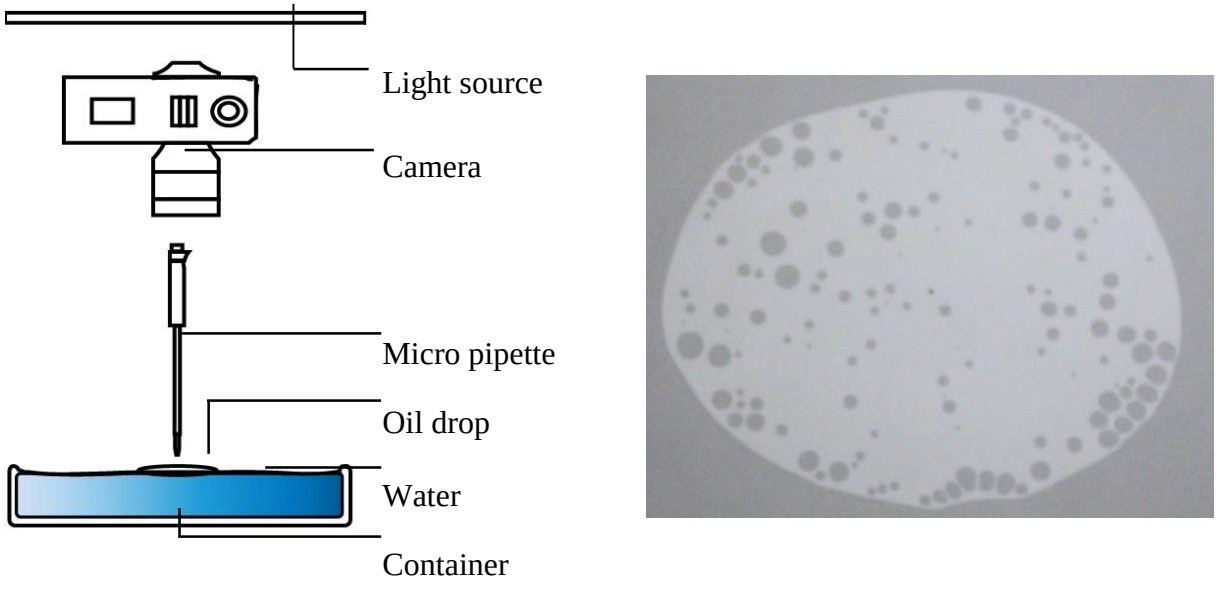

Figure 1: (a) Schematic of the experimental setup, (b) Raw image of the coconut oil film on water at 120 seconds after the start of the experiment.

Experiments were performed with four different natural oils viz.,Sesamumindicum (sesame oil), Olea europaea (olive oil), Cocos Nucifera (coconut oil) and Ricinuscommunis (castor oil). A Siemens SG series Ultra ClearTM water deionization system was the source of the deionized water. The water conductivity was less than 1.5$\mu S/cm$, indicating a high level of purity. A drop of natural oil was placed on the surface of the substrate fluid. Natural oil drop spreads on surface of water because the spreading co-efficient in all instances was positive. The spreading patterns of the oil film were imaged using a Canon 600D DSLR camera with an EOS 18-55mm lens at a rate of about three frames per second. Each frame had a spatial resolution of 16 megapixels. Two Light Emitting Diode (LED) backlights are used as sources of illumination to image the oil pattern formed on the aqueous free surface. The camera was placed above the container to view the water surface as shown in figure 1(a). Camera which was tilted to an angle (approximately 20°) to the vertical in order to complete view of the total water surface of the container. After conducting every experiment, the water container was rinsed using isopropyl alcohol and then cleaned with water. Further for every experiment the tip of the micropipette is changed. The container was completely sponged with lint free tissue paper. Experiments were performed in a controlled environment. The humidity and temperature was controlled in this case. It was also ensured that there is only little circulation of air in the room. Because air circulation affects the spreading rate of natural oil.

https://doi.org/10.64151/PSGCARE-13

ISSN 2394 - 9554

Table 1: Interfacial tension of substrate and drop fluids. Surface tensions of natural oils were measured using duNuoy ring method. All other data were measured by the pendant drop method.(The data of Coconut Oil-1 is adapted from Swaminathan and Panchagnula[5])

Substance	Surface tension (mN/m)	Interfacial tension with water (mN/m)	Harkin's spreading coefficient (*S*, mN/m)	Viscosity (cSt)	Density (kg/m^3)
Coconut oil-1	28 (±0.2)	5.6 (±0.4)	36.4	27.71	924
Coconut oil-2	28.5 (±0.2)	11.31(±0.7)	30.2	27.71	924
Coconut oil-3	29 (±0.2)	12.9(±1.2)	28.1	27.71	924
Olive oil	29.75	15.86(±1)	24.4	24	918
Gingelly Oil (Sesame oil)	28.1	14.64(±1.6)	27.3	39.9	919
Castor Oil	35.1	12.8(±1.5)	22.2	325	961
Substrate (Water)	70	70	--	1	980

The chemical composition of all the oil samples was tested using a Gas Chromatography Mass Spectrometry (GCMS) system. The data from those measurements are reported hereunder in Table 2. Let us first consider the three samples of coconut oil investigated, marked as 1, 2 and 3 in the Table 2. As can be seen, most of the constituents occur in approximately the same quantity. Subtle differences of the order of less than 10% persist in some of the minor constituents, which can only be detected by GCMS. In cases, where such detailed quantitative information is not required but only whether the oil has changed, it is expensive to conduct such an experiment. An unique technique will be discussed based on an experiment where an oil drop spreads on water to discover a measurable effect of these subtle differences in chemical composition.

Table 2: Chemical composition of natural oils.(The data of Coconut Oil-1 is adapted from [5])

https://doi.org/10.64151/PSGCARE-13

ISSN 2394 - 9554

Natural Oil / Fatty acid	Coconut Oil-1	Coconut Oil-2	Coconut Oil-3	Olive Oil	Castor Oil	Gingelly Oil
C8:0	8.87	10.11	9.77	0.00	0.00	0.00
C10:0	5.17	5.94	6.20	0.00	0.00	0.00
C12:0	42.04	43.32	47.04	0.00	0.00	0.00
C14:0	20.02	17.84	18.45	0.01	0.01	0.03
C16:0	8.94	12.60	7.63	13.04	2.05	9.11
C16:1	0.00	0.00	0.00	1.28	0.00	0.14
C18:0	3.43	1.29	2.53	2.75	1.79	43.45
C18:1	8.33	4.83	6.24	71.53	5.88	39.17
C18:2	2.29	.81	1.66	9.76	7.59	0.29
C18:3	0.16	0.45	0.18	0.54	0.67	0.71
C20:0	0.00	0.00	0.00	0.45	0.00	0.15
C20:1	0.00	0.00	0.00	0.27	0.41	6.69
C18:1-OH	0.00	0.00	0.00	0.00	81.59	0.00
Others	0.00	0.00	0.31	0.10	0.00	0.28

RESULTS AND DISCUSSION

The common physical observations from all four natural oils. The oil film evolution is through following three main phases – (i) spreading, (ii) hole inception and hole growth and (iii) hole coalescence, which results in oil film coarsening. Holes are observed to nucleate on the spreading film, primarily near the rim of the spreading oil film. Figure 2 is used to discuss these aspects. Figure 2 shows modified color representation of the spreading oil film from four different natural oils - gingelly oil, castor oil, olive oil and coconut oil drop on water. Brown color indicates oil films and light blue color indicates water. Images (a), (e), (i), (m) are at 15s, (b), (f), (j) and (n) are at 60s, (c), (g), (k) and (o) are at 120s and (d), (h), (l) and (p) are at 210s.

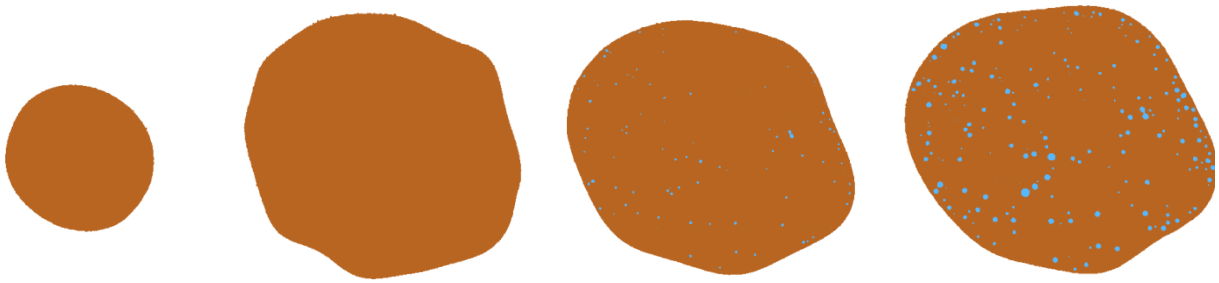

https://doi.org/10.64151/PSGCARE-13

ISSN 2394 - 9554

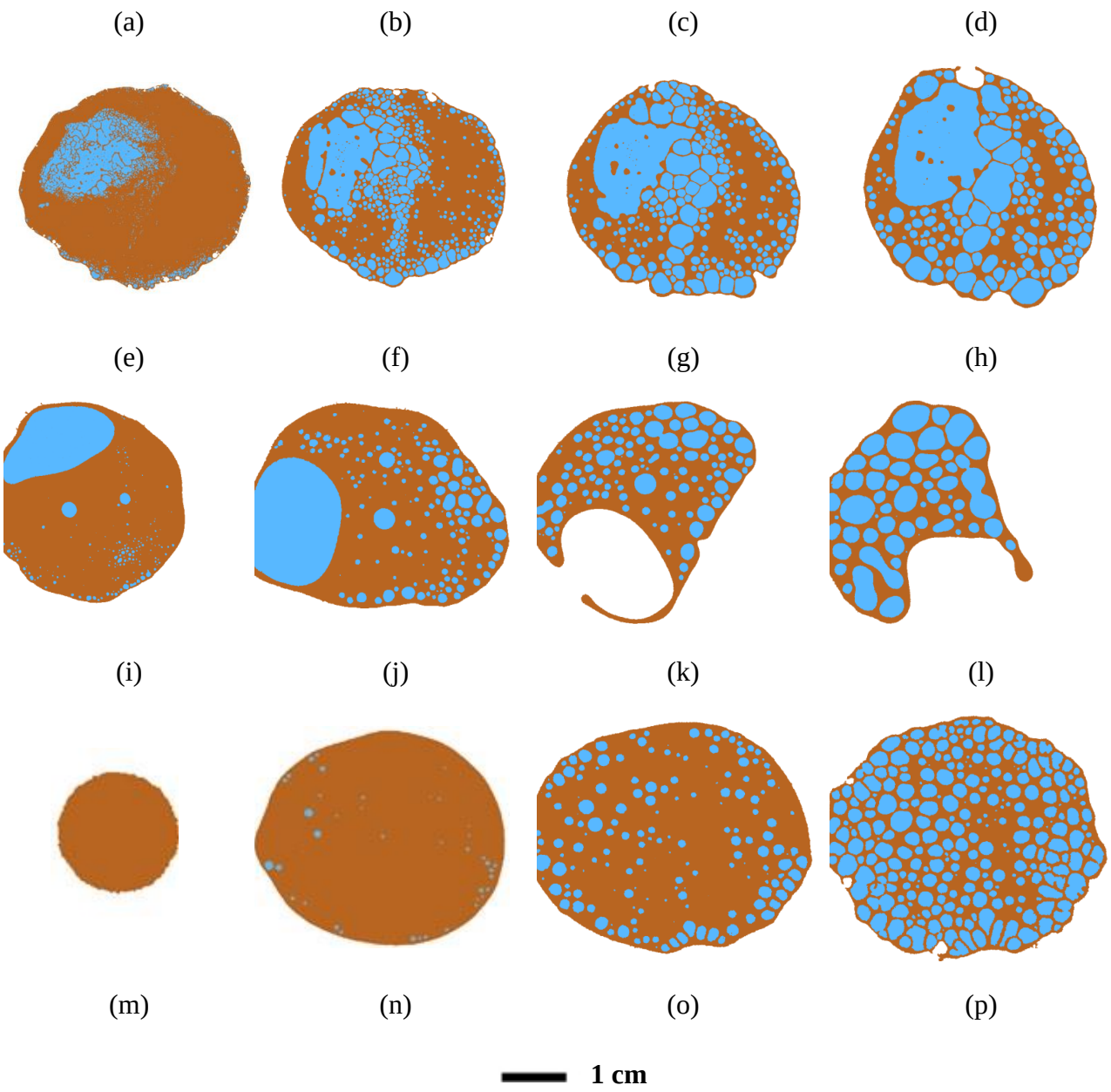

Figure 2: Images of the oil film from (a-d) gingelly oil, (e-h) castor oil, (i-l) olive oil and(m-p) coconut oil drop spreading on water surface. Images (a), (e), (i), (m) are at 15s, (b), (f), (j)and (n) are at 60s, (c), (g), (k) and (o) are at 120s and (d), (h), (l) and (p) are at 210s.

As the oil drop is placed on the free surface of water, an oil film of increasing diameter is formed. In Figure 2 Blue indicates water and brown indicates oil. This can be observed in Figure 2(b) and 2(c) which is images is obtained after 60 and 120 seconds, respectively, from the instant when the oil drop is placed. In the case of gingelly oil shown in the figure 2(a) – (d) it was found that hole nucleation is very slow. The nucleated hole increases in diameter due to the fact that oil dewets the water free surface . This is similar to the phenomena observed by previous researchers[6]. The hole increases in diameter until its

https://doi.org/10.64151/PSGCARE-13

ISSN 2394 - 9554

growth affected by the presence of the nearby holes.

During the hole coalescence the liquid bridge which separates the holes breaks and this process, facilitates the progression of oil film coarsening. Hole coalescence in different oils such as olive oil, coconut oil and castor oil were shown in the figures. Figures 2(i) and 2(k) show images of the olive oil spreading on water. Here, it shows that the process of coalescence has caused the mean hole size to increase. At all later time (for example, see Figure 2(l)), the oil films (which was a continuous thin liquid sheet) are reduced to cellular patterns of oil film. Since this process is spontaneous, it requires no external input. The complete spreading and the dynamical processes takes about 2 hours to attain the steady state of fully emulsified oil drops on water.

The oil film dynamics can be quantified using three parameters. The total perimeter length separating the oil and water phases is calculated following our previous work (Swaminathan and Panchagnula[5]).This quantity is an indication of the degree of engagement between the oil and water phases. Secondly, the total number of holes on the oil film as a function of time is can be used as a measure of the surface activity of the oil. Finally, we have characterized an individual hole growth characteristics, which will serve as the final marker for adulteration detection.

The dynamics of the rate of total triple line length is discussed next. The total triple line is measured as the total length of the curve separating the oil film and the substrate water. This includes the perimeter surrounding each hole as well as the outer diameter of the oil film. Figure 3(a) is a plot of the total perimeter versus time for a drop of coconut oil spreading on water. The data in this figure was obtained from three trials of the experiment (error bars indicate the variation from trial to trial). The total triple line length in this figure increases gradually initially (till about 10 seconds). Subsequently, it increases rapidly reaching a maximum at about 100 seconds. After this instant of time, the total triple line length begins to decrease. In addition, it can be observed from the lengths of the error bars that the repeatability of the experiment, especially at the maximum triple line length condition is very good (< 1%). Figure 3(b) shows the variation of triple line length(P)with respect to time for a coconut oil drop spreading on water. Three samples obtained from three different sources have been included in this figure and their chemical compositions are indicated in Table 2. Even though the differences in chemical composition are very subtle, the triple line dynamics, especially near the maximum triple line condition are different. Therefore, the total triple line length is chosen as a good marker to examine oil quality.

https://doi.org/10.64151/PSGCARE-13

ISSN 2394 - 9554

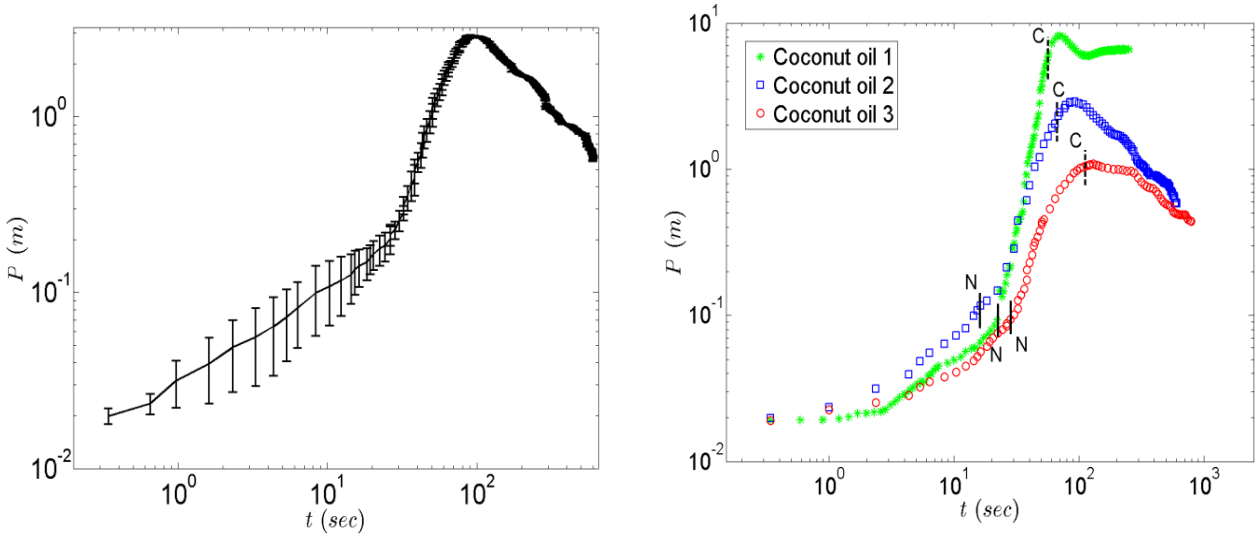

Figure 3: Plot of total perimeter versus time for coconut oil spreading on water. (a) Error bars are indicated to show the error in repeatability from three trials.(b) Plot of total perimeter of coconut oil obtained from three different sources.

Figure 4 depicts a plot of the triple line length (P) characterizing the spreading process with each of the four different oils. Two small vertical lines are added in each data series. These small lines signify the time at which there is a new physical process. In the Figure 3, a vertical line named as N shows the time at which there a first hole on the spreading oil film. Similarly, C indicates the instant at which the hole count (in Figure 4) shows a maximum. After the hole count attains a maximum, coalescence events occur in greater frequency. The time duration before the instant N corresponds to the phase where a spreading oil film is observed. In between the time instants N and C hole inception and growth dominate. Finally, for times after the instant C, hole coalescence dominates the oil film dynamics. Three different inferences are made using the data shown in Figure 4. Firstly, the triple line length initially scales as $t^{0.5}$in keeping with the coconut oil film and gingelly oil film and slightly higher for olive oil and castor oil. First hole inception causes a sudden change in the slope of the triple line length of different oil samples. During this phase $P \sim t^m$ with $m = 0.6$ for Castor oil and, $m = 0.7$ for Gingelly oil and $m = 0.6$ for Olive oil and $m = 2.3$ for one type of coconut oil. The value of m changes with the nucleation rate for different oils. Total triple line length gives the general information in the evolution of the process. It was also observed that there is a change in the total triple line rate when there is a change in the phase of the evolution of the process. After the hole formation and hole growth regime, the oil film dynamics changes into a different phase, In this phase, more coalescence events at the instants 'C' in the Figure 4. During this stage a decrease in total triple line length rate was observed as showed in Figure 4. At the end of this stage, oil film evolves into cellular patterns (with large holes and thin rims), which further breaks down into drops due to Rayleigh-Plateau instability.

https://doi.org/10.64151/PSGCARE-13

ISSN 2394 - 9554

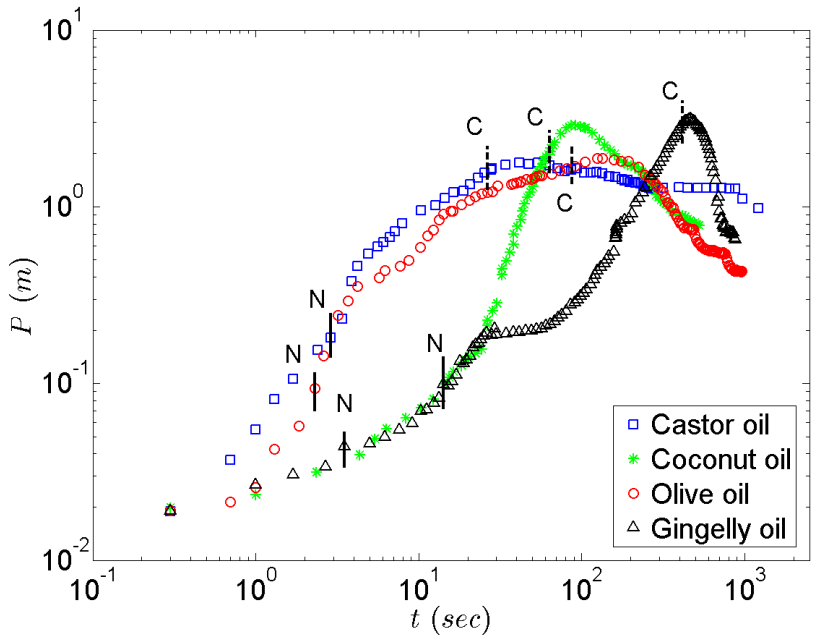

Figure 4: Change in perimeter of different natural oil at different time steps (log-log plot). The triple line is defined as the curve distinguishing the oil and water phases.

The maximum value of P (in Figure 4) for the coconut oil experiment is around 3m but at the same time the oil film diameter is around 90mm. This shows that an oil film with small surface area was very tightly packed with over 1000 holes, and the rim of the holes has the thickness of the order 1mm. The maximum triple line length changes if there is a change in the type of oil. Therefore, I would like to reiterate that this quantity is a sensitive quantity to identify the type of oil as well as adulteration.

From the figure 5 it is found that the oil film diameter of the four samples is considerably different in the course of the spreading phase. But when the same spreading rate is collapses in to single curve with small deviation, when it is multiplied with viscosity ratio (of Oil and water) and divided with spreading coefficient of the corresponding oil.

https://doi.org/10.64151/PSGCARE-13

ISSN 2394 - 9554

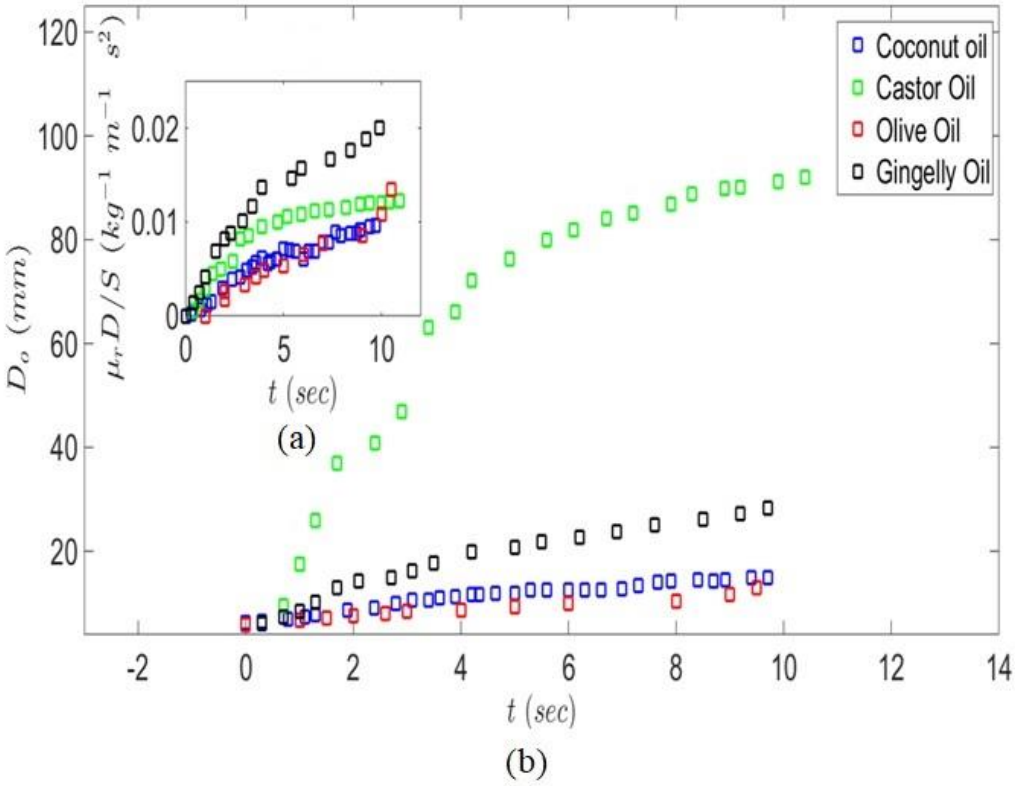

Figure 5:(a) Plot of Outer diameter of the spreading diameter (D_O) versus time of different oils viz. coconut oil, Castor oil, Olive oil and Gingelly oil. Inset plot shows the plot of modified spreading velocity. The spreading velocity is modified with viscosity ratio and spreading coefficient of the corresponding oil $m = \frac{\mu_r D}{\sigma}$. Then this modified diameter is subtracted with initial modified diameter $(m - m_o)$.

Hole nucleation and its growth is key to the increasing surface area. Figure 6 is a plot of the variation of individual hole diameter in time. The diameters of several similar holes are monitored and data for a representative hole are presented in this graph for each oil. it was made sure that the data was repeatable. As we mentioned before the triple line length is calculated as the sum of the perimeter of each hole as well as the outer diameter of the oil film. The sharp increase in triple line length observed after about 10 seconds is a result of two physical phenomena – a sudden increase in hole count (already discussed in the context of Figure 5) and the growth of the perimeter of each hole, which is related to its diameter. The latter data is presented in Figure 4.

The diameter of single hole growth of olive oil, gingelly oil, castor oil and coconut oil was observe to follow a power law and shows a trend line with an exponent of 0.45, 0.22, 0.44 and 0.5 respectively. While castor oil, coconut oil and olive oil are somewhat similar in their trends, gingelly oil is distinctly slower. This indicates that gingelly oil has a significantly slower surface activity, which deserves further investigation.

https://doi.org/10.64151/PSGCARE-13

ISSN 2394 - 9554

The sharp rise in the total triple line length after about 10 seconds is due to the nucleation and growth of holes on the oil film. We will now turn our attention to discuss Spreading rate Figure 5 shows the change in spreading front with respect to time.

Capillary number $Ca = \frac{\mu v}{\sigma}$ variant to modify the diameter with viscosity and spreading coefficient.

$$\text{Modified diameter (for different oil)} = \frac{\mu_r D}{\sigma} \rightarrow 1$$

$$\text{Viscosity ratio } \mu_r = \frac{\mu_w}{\mu_o} \rightarrow 2$$

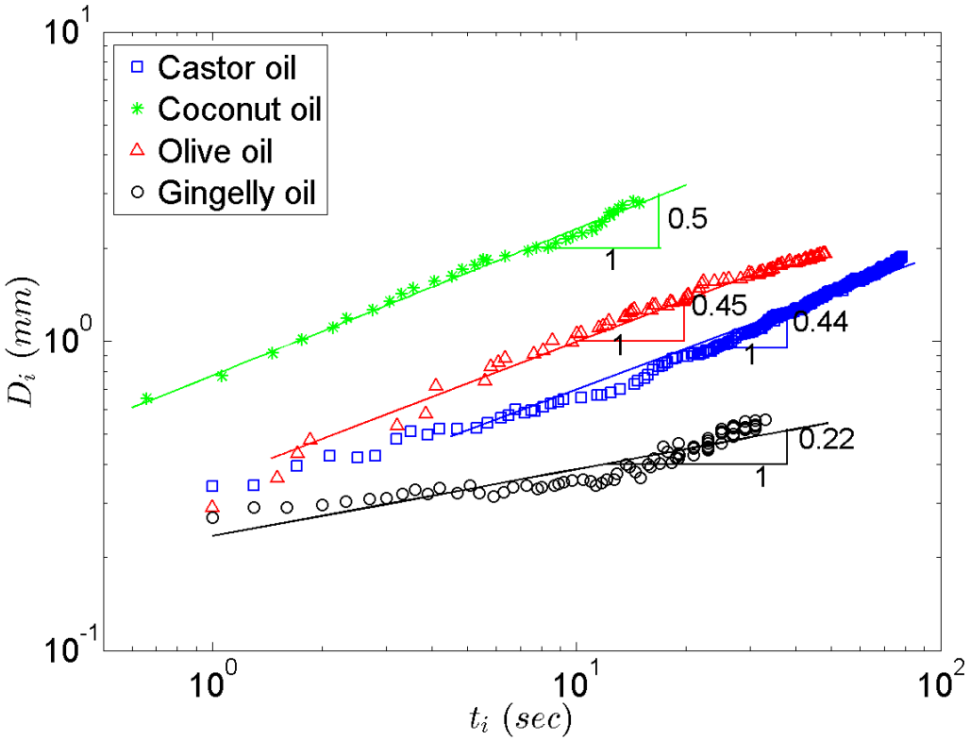

Figure 6: Plot of hole diameter (D_i) versus time. The hole diameter is measured for a single hole to characterize its growth. Spreading of coconut oil shows that $D_i \sim t_i^{0.5}$. All other experiments show $D_i \sim t_i^{0.45}$, $D_i \sim t_i^{0.44}$ and $D_i \sim t_i^{0.22}$ for Olive oil, Castor oil and Gingelly oil respectively.

The spreading front of the oil tends to push the water free surface which is detected by the movement of particle kept near the oil drop. When the spreading front is large enough this spreading front's effect reaches the wall of the container. Figure 7 (a) and (b) shows the velocity vectors of the path traced by the centroids of all the holes formed. From the figure it was found that the whole free surface tends to rotate in a direction depend on the spreading front of the oil drop. The path lines of all the holes initially behaves like source flow but towards the end of hole formation regime. Path of the holes twisted in a clock wise direction and further follows the outer spreading fronts shape profile.

https://doi.org/10.64151/PSGCARE-13

ISSN 2394 - 9554

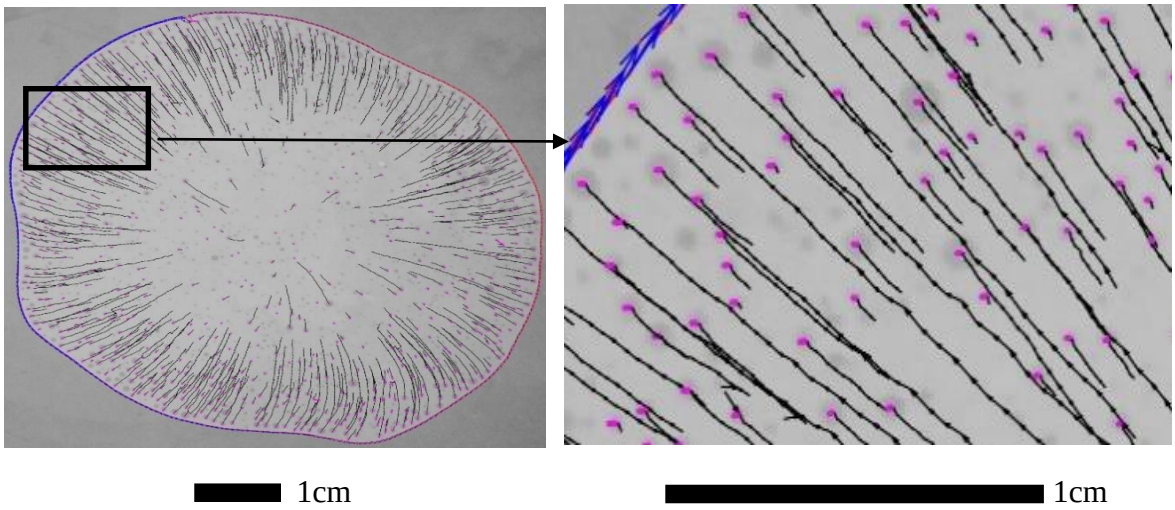

Figure 7 (a): Black arrows shows the individual path lines of all the hole formed in the spreading front of the oil. (b) the zoomed view of the velocity vectors of the holes.

Similarly, when the path traced by a all the holes shows that the nucleated holes are following the spreading fronts behavior. Figure 8 (a) show the plot between hole displacement of a single for every timestep and spreading front area. This graph shows that the hole displacement of the first hole is slightly increased and then decreased. Figure 8 (b) show the plot between hole displacement of all the holes for every timestep and spreading front area. The graph shows that, the displacement of the holes shows that the distance travelled by the initial holes are low and comparatively increases and then decreases and reaches a constant distance. Furthermore, the change in hole displacement is not smooth. Throughout the hole nucleation regime, the hole displacement is in continuously zigzag motion. This randomness increases with the increase in spreading area. Increase in number of holes increases the randomness of the system.

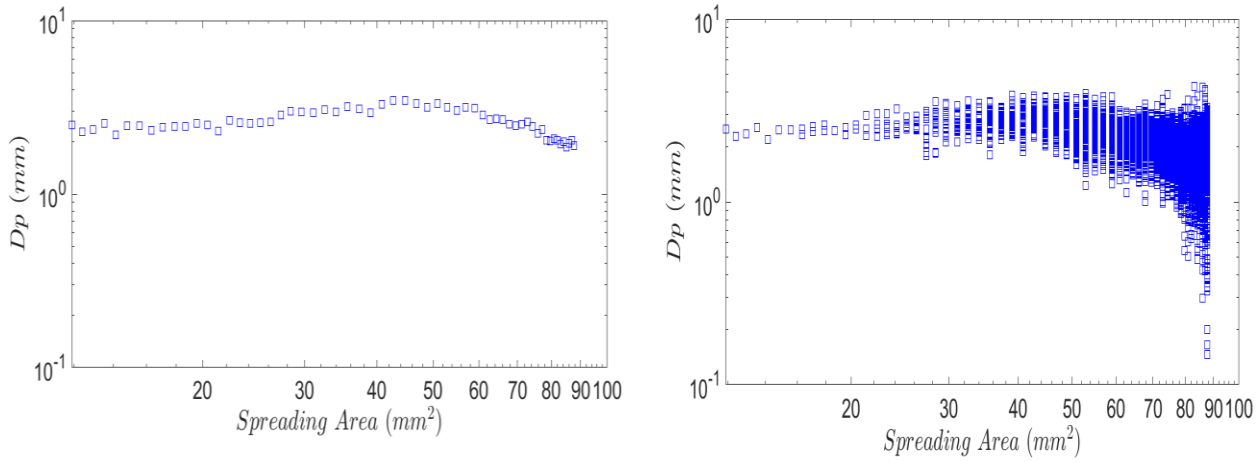

(a) (b)

Figure 8: (a) Hole displacement of a single the holes at every time step vs spreading front area.

https://doi.org/10.64151/PSGCARE-13

ISSN 2394 - 9554

b. Hole displacement of all the holes at every time step vs spreading front area

The spreading front of coconut oil is modelled as source flow. The strength of the source term is of the order of area of the spreading front in water surface. Therefore, strength of source term is taken as area of the oil spreading front with a coefficient of area. Similarly, hole formation processes are modelled as source flows, here the strength of the source term is taken as a area of the hole formed with a coefficient. This model exactly captures both the spreading front and hole formation process till the hole formation regime. A microscopic image of single hole formation and the movement of the grid due to the influence of source flow is shown in the figure 9 (a) and (b). It shows that the grid movement due to the source flow and the microscopic image of a single hole matches well. In figure 9 (b) red circle was plotted by taking hole area of the microscopic image. It was also observed that there is a distortion in the microscopic image of the hole in the radial direction due to the effect of spreading front as shown by arrows in the figure 9(a).

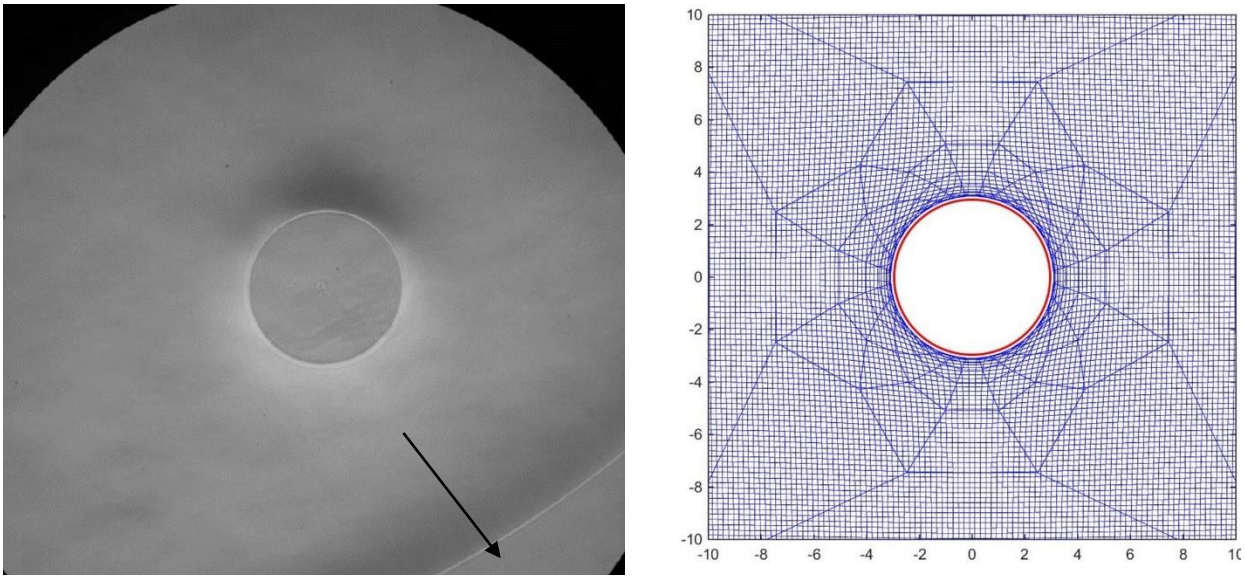

Figure:9 (a) Microscopic image of single hole in the oil spreading front (b) Movement of adjacent grid points due to a single source term in the centroid.

All the holes are modelled as a source flow with the source strength of a corresponding hole area's order. Then the summation velocity is calculated. It was found the source terms near the boundary of the spreading front had greater effect on the profile of the spreading front. Streamlines drawn were drawn with the velocity field of source flow of the spreading front and source flows of the individual holes. Streamline is also a function of flowrate therefore using the width between the streamlines and the length of the corresponding streamlines gives the flowrate in that area. Using that calculated flowrate the spreading front profile is constructed. It shows that the constructed spreading front profile is well predicting the actual shape profile of the spreading front. Since the oil/water interface has a no slip condition. Even an infinitesimal shear will create a flow. Here flow of the oil is created by spreading coefficient. This flow of oil spreading front also moves the adjacent water free surface. This can be observed by keeping a small particle near the oil drop.

https://doi.org/10.64151/PSGCARE-13

ISSN 2394 - 9554

Figure 7 shows the model able to predict the shape and the size of the formed hole. There are some discrepancies in modelling the location of the hole.

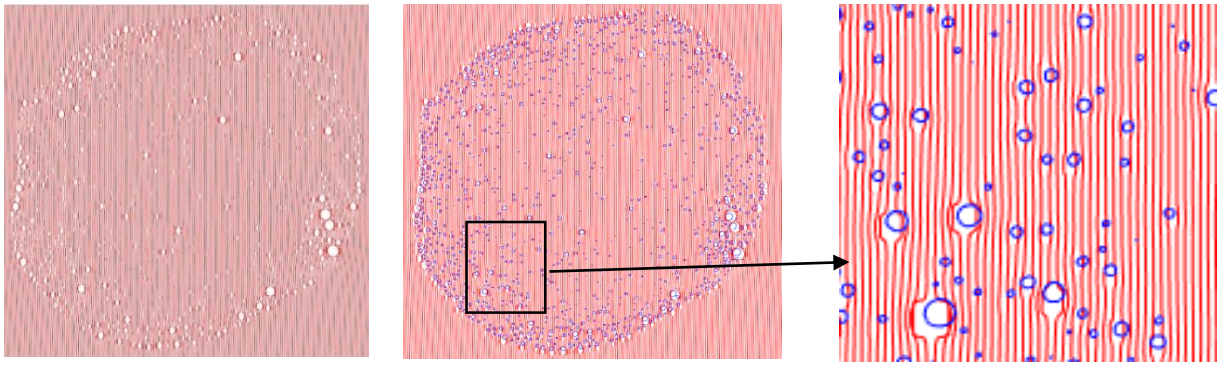

Coordinate movement due to the effect of modelled hole formation

Comparison of the effect of modelled hole formation and actual hole formation

Zoomed view of the movement of coordinates due to the effect of modelled hole formation and actual hole formation

Figure 10: Hole formation effect is modelled as source flow and plotted with actual plot of hole coordinates.

Figure 10 (a),(b),(c)shows the plot of the coordinates of all the holes with the modelled holes as source flow terms. From the figure it was found that there is discrepancy in the movement of grid points due to source flow and the plot of the hole coordinates. This is due to the face that the center of the hole is a singularity, velocity vectors are calculated few points away from the centroid of the hole. Because of this velocity vectors were calculated in such a way that center exists in equidistance from the adjacent grid points. Because of this there is some distortions in the locations of the model and the actual location of the hole.

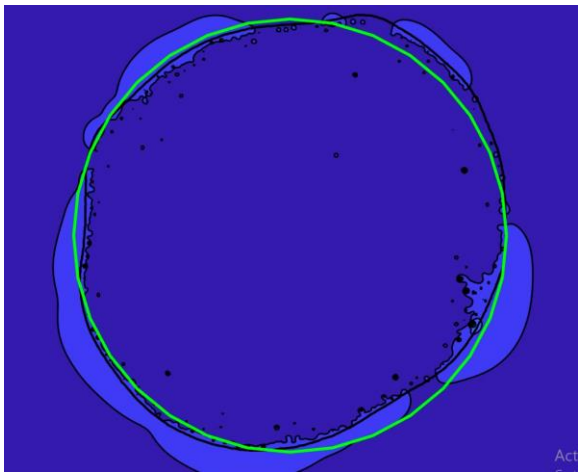

Figure 11: Contour plot of the velocity vectors affecting the spreading front's shape profile when more number of holes formed along the periphery of the spreading front.

https://doi.org/10.64151/PSGCARE-13

ISSN 2394 - 9554

Figure 11 shows the pseudo color images of the velocity of all the modelled holes. It was found that the velocity gradients with the effect of wall are predicting the meniscus movement to some extent. Now to analyze the movement of the meniscus is modelled by considering the meniscus using the immersed boundary method. Here the meniscus is considered as a rubber band. The viscosity of the spreading liquid is used as a shear stress. Tensile stress is modelled using the value of surface tension of the spreading liquid.

Figure 12 depicts pseudo color depictions of the oil film morphology at the condition when the triple line length is maximum. As can be seen, the dynamics at this condition are very different for each of the oils. In addition, the actual lengths of the triple line also vary significantly. Therefore, I would like to submit that this parameter is a key indicator both of oil quality (in terms of adulteration) as well as oil type. The image of the oil film at and near this condition could be used as markers for quality control.

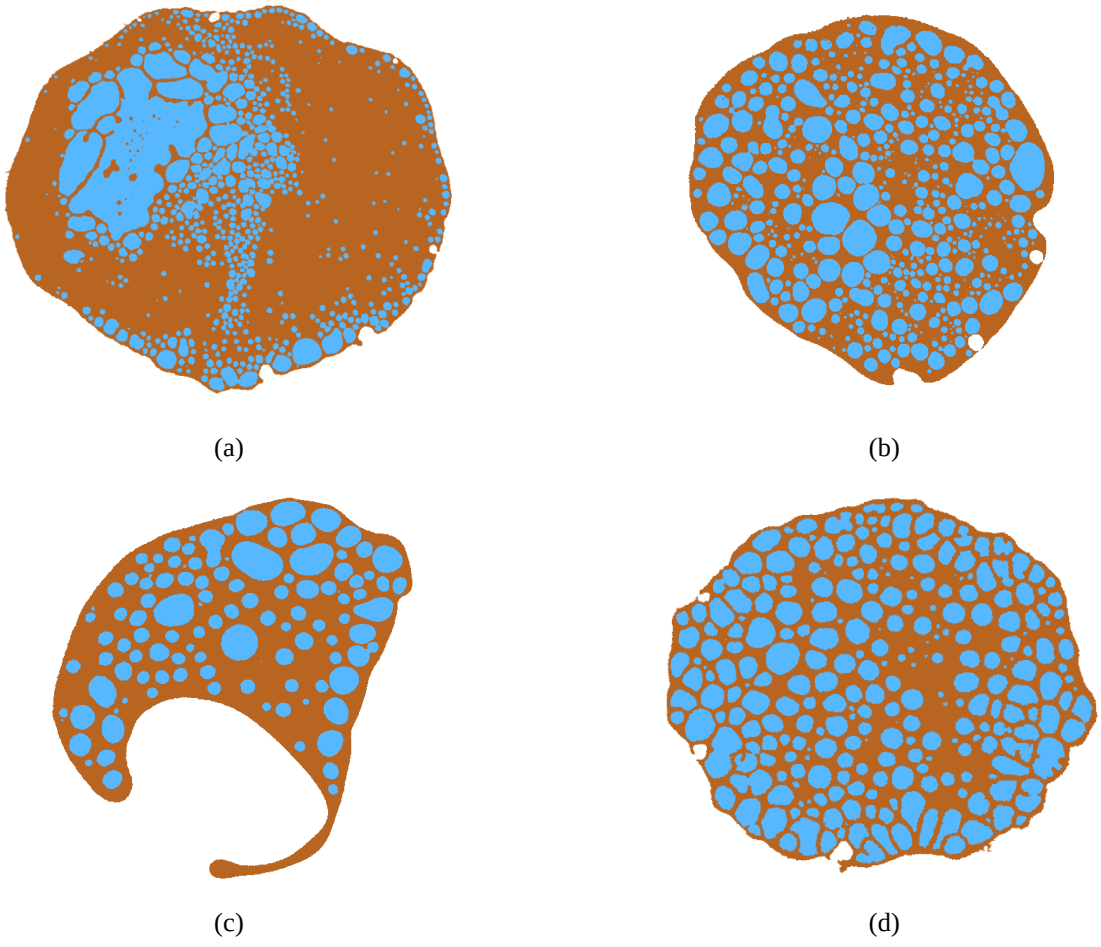

https://doi.org/10.64151/PSGCARE-13

ISSN 2394 - 9554

Figure 12: Images depicting the oil film morphology at the instant(s) when the total triple line length is maximum for (a) Castor oil ($P = 1.776m$ at this condition), (b) Gingelly oil ($P = 3.125m$ at this condition), (c) Olive oil ($P = 1.88m$ at this condition) and (d) Coconut oil ($P = 2.88m$ at this condition). The ratio of the triple line length to the oil film diameter in these cases is on the order of 10^2, indicating the high degree of emulsification.

CONCLUSION

We study the behavior of a film of natural oil on water. The objective of the study was to identify marker parameters, which can be used for quality control. Natural Oils like Coconut oil, Gingelly oil, Olive oil, and Castor oil have also been used as the drop fluids. The experimental apparatus allowed for the imaging of the oil film during the course of its evolution. The general behavior of the oil film from all four oils was observed to be similar. The dynamics was initially dominated by a phase where the oil film continued to spread on water. At a later instant of time, holes were observed to nucleate on the film. These holes increased both in number as well as in their diameters. At a much later instant, it was observed that these holes would begin to coalesce to form bigger holes.

Our experiments with natural oil on water showed that each oil has a different spreading pattern during the hole nucleation and growth phase. From a systematic study, total triple line length is identified as a marker parameter for ensuring oil quality. In this regard, triple line length is nothing but the span of a curve separating the oil and water regions of the film. The greater the length of this line, the greater is the degree to which the two phases (oil and water) are mixed. Similar experiments have been performed with coconut oil obtained from different sources. These experiments show that coconut oil having a unique chemical composition has a unique nature of triple line at the maximum emulsification condition. Finally, we conclude that the spreading pattern obtained with a particular sample of oil on water carries information related to its chemical characteristics and hence can be used to identify the oil.

ACKNOWLEDGEMENT:

KS would like to acknowledge Prof. Mahesh V. Panchagnula from IIT Madras for useful conversations and use of lab facilities.

REFERENCES

1. T. Hoshino, M.-W. Liu, K.-A. Wu, H.-Y. Chen, T. Tsuruyama and S. Komura, Physical Review E **99** (3), 032416 (2019).
2. T. K. Jose and K. Anand, Fuel **177**, 190-196 (2016).
3. S. Babu, R. V. Sudershan, R. K. Sharma and R. V. Bhat, JAOCS, Journal of the American Oil Chemists' Society **73** (3), 397-398 (1996).
4. W. D. Harkins and A. Feldman, Journal of the American Chemical Society **44** (12), 2665-2685 (1922).
5. K. Swaminathan and M. V. Panchagnula, Colloids and Surfaces A: Physicochemical and Engineering Aspects **520**, 796-804 (2017).
6. R. Yerushalmi-Rozen, T. Kerle and J. Klein, Science **285** (5431), 1254-1256 (1999).

https://doi.org/10.64151/PSGCARE-13